Field-Scale Estimation of Volumetric Water Content using GPR Groundwave Techniques

K. Grote [1], S. Hubbard [2], Y. Rubin [1]

[1] Dept. of Civil and Env. Engineering, UC Berkeley, Berkeley, CA 94720 krgrote@lbl.gov

[2] Lawrence Berkeley National Laboratory, Berkeley, CA 94720

Abstract

Ground penetrating radar (GPR) groundwave techniques were applied to estimate the soil water content in the uppermost ~15 cm of a California vineyard several times over a year period. Densely spaced GPR measurements were collected at 900 MHz and 450 MHz, and both travel time and amplitude data were analyzed to estimate water content. The GPR estimates of water content were compared to gravimetric water content, soil texture, and time domain reflectometry (TDR) measurements. Comparison of the water content values estimated using GPR groundwave data with gravimetric water content measurements showed that the GPR estimates were accurate and that the vertical distribution of water content could be inferred using multi-frequency GPR data. The pattern of spatial variability of water content across the vineyard derived from GPR estimates did not change significantly with time, although the absolute water content values varied seasonally and with irrigation. The spatial variations in water content at this site appear to be controlled by soil texture. Analysis of TDR data using 15 cm probes produced estimates of water content that agreed well with those obtained from GPR measurements, which suggests that at these GPR frequencies, the two techniques have comparable sample volumes and measurement accuracies. The comparisons of GPR-derived estimates of water content to gravimetric water content and TDR measurements show that GPR

groundwave techniques can be used to provide quick, accurate, spatially dense, and non-invasive estimates of shallow water content in large-scale field applications.

1. Introduction

Monitoring of near-surface soil water content is a vital component for agricultural, ecological, meteorological, and vadose zone programs and for rational water resources management. The information obtained from monitoring water content at agricultural sites is critical for optimizing crop quality, achieving high irrigation efficiencies, and minimizing lost yield due to waterlogging and salinization. Water content monitoring is also important for addressing issues of water quantity and quality, both relevant for managing the environmental impacts of irrigated agriculture and for protecting functional ecosystems. Finally, water content is an important parameter for understanding vadose zone processes such as evapotranspiration and partitioning of precipitation into surface runoff or groundwater storage and as input into meteorological models.

For precision vineyard management, knowledge of the soil water content is essential for optimizing fruit quality. If too much water is applied, fruit quality is decreased and roots can be damaged by waterlogging, but too little water stresses the plant and can damage both the fruit and the vines (Williams et al., 1994). Additionally, natural variations in water content across a vineyard may contribute to differences in the vigor of the vegetation. Precision vineyard management strives to tailor farming practices such as irrigation, fertilization, and harvesting throughout a field based on variations in parameters such as vigor (Johnson et al., 2000). The water content in the root zone, usually from the ground surface to a few meters depth, is of most importance to viticulturists, and the critical range of water content is from the wilting point, or the water content below which plants cannot be revived, to approximately half the water content

at saturation. Although the wilting and saturation points vary for each soil, the range of volumetric water content (the volume of water in a soil sample divided by the total volume of the sample) of interest in most agricultural soils is from ~0.10 to ~0.25 (Pritchard, 1999). In addition to using shallow soil water content information to improve fruit quality and irrigation efficiency, preliminary knowledge of soil water content ranges and spatial patterns prior to planting could be used to optimize vineyard layout.

Viticulturists currently use several conventional tools to assess the moisture status of the soil, including gravimetric sampling, time domain reflectometry (TDR), frequency domain reflectometry, neutron probe logging, tensiometers, and electrical resistance and thermal dissipation in porous blocks. Water content estimates from these tools are often used to decide the scheduling and quantity of vineyard irrigation (Pritchard, 1999). However, near-surface water content is a function of properties such as topography, precipitation, evapotranspiration, geology, and vegetation, and these properties are spatially and sometimes temporally variable (Western et al., 1998). Because of this heterogeneity, collection of enough point measurements to adequately capture the spatial trends of water content within a vineyard is difficult. Additionally, conventional point measurements are invasive and disturb the soil structure, and thus the measurements obtained may not represent in-situ moisture conditions.

An alternative to conventional methods is remote sensing, which uses infrared and microwave frequencies to estimate water content in the uppermost 0-5 cm of soil (Jackson et al., 1996). Remote sensing techniques permit estimation of water content quickly and over very large areas, but typically provide poor resolution; the highest resolution possible from spaceborne sensors is on the order of 100 m (Jackson et al., 1996; Mancini et al., 1999). As remote sensing measurements are affected by factors such as surface roughness, vegetation,

illumination geometry, and system parameters (Mauser et al., 1994), these measurements must be calibrated before conversion into water content estimates. Finally, crop cover can prevent the use of remote sensing for estimating water content in crops that have full leaf canopies when mature, so these measurements are effective only when the crop is in an emergent state (Pultz et al., 1990). These limitations reduce the effectiveness of remote sensing techniques for providing high-resolution soil water content information in applications such as precision agriculture.

Near-surface geophysical techniques have been used to obtain water content estimates at spatial scales in between those of conventional point measurements and remote sensing data. Electrical methods are well established for mapping the values and spatial distribution of soil water content (Kean et al., 1987; Frolich and Parke, 1989; Luck and Eisenreich, 2001), and low-frequency electromagnetic methods (Sheets and Hendricks, 1995) have also been used successfully for this purpose. However, these techniques may produce inaccurate results if data are collected near metal structures, such as the metal stakes and trellis wires found in most vineyards. Additionally, both electrical and low frequency electromagnetic measurements may be time consuming to collect, require interpretation and calibration, can be sensitive to temperature, and may have low resolution compared to the scale of heterogeneity of near-surface water content.

Our research focuses on investigating the applicability of another geophysical technique, ground penetrating radar (GPR), for use as a field water content estimation tool. In this paper, we concentrate on information obtained from GPR groundwaves, which probe only the shallow subsurface. As the GPR groundwave measurement depth is partially a function of frequency, groundwave data can also be used to estimate the near-surface water content profile by comparing data collected at different frequencies. GPR groundwaves have the potential to

quickly provide water content estimates with a vertical resolution comparable to that of conventional methods, but with much greater lateral resolution, leading to a better estimation of water content over large areas and to an improved understanding of the three-dimensional variability of water content within an area.

The goals of this experiment were to develop data collection and interpretation techniques that provide accurate, rapid estimates of near-surface water content using GPR groundwave travel time and amplitude data, to validate and calibrate GPR-obtained water content estimates through comparison with conventional point-based measurements including gravimetric sampling and TDR, and to compare GPR estimates of water content with soil texture data. After development of data acquisition and interpretation techniques, we apply GPR groundwave technology to a heterogeneous field site at the Robert Mondavi Winery in Napa, California to estimate temporal and spatial variations in water content under natural field conditions. A brief background of water content estimation methods using GPR groundwaves is given in Section 2, and the site description and data collection procedures for this experiment are presented in Section 3. Section 4 describes the data interpretation and validation techniques and the correlations between the different types of measurements, and Section 5 shows the results of applying the data interpretation techniques to estimate water content across the entire field site at different times during the year.

2. Background of GPR Groundwaves

GPR is a geophysical technique that uses high frequency (50-1500 MHz) electromagnetic energy to probe the subsurface. At these frequencies, the electrical response is dominated by the dielectric properties of a material, where the dielectric properties are characterized by the polarization of opposite electric charges in a material subjected to an external electric field

(Davis and Annan, 1989). GPR techniques generally are most effective in coarse or moderately coarse-grained unsaturated soils and may perform poorly in soils with saline pore fluid or a large component of swelling clays.

GPR groundwaves are boundary waves that are created by the contrast in electromagnetic velocity between air and near-surface materials. Energy is emitted from the GPR transmitter as a spherical wave, and some of this energy travels along the air-ground interface in the near subsurface to the receiver; this energy is referred to as the groundwave. A more complete description of the groundwave is given by Berktold et al. (1998). In addition to the groundwave, other energy that travels directly from the transmitter to the receiver is the airwave, which is a wave traveling in the air at the speed of light. The groundwave travels at a velocity (v) determined by the properties of the near surface materials. For agricultural applications, the near surface material is usually soil, and water content typically has the most influence on the velocity of unsaturated soils. The approximate depth of influence of the groundwave (z), or the thickness of the zone between the ground surface and the maximum penetration depth of the groundwave, is determined as half of the Fresnel zone for seismic waves (Hagedoorn, 1954). This approach was later adopted by Van Overmeeren et al. (1997) for use with GPR groundwaves; they expressed the depth of influence as:

$$z = \frac{1}{2}\sqrt{\frac{vS}{f}} \ , \tag{1}$$

where f is the central frequency of the GPR signal and S is the separation distance between the transmitting and receiving antennas. This expression indicates that the depth of influence of the groundwave is greater in dry soils, which have higher velocities, than in wet soils, and signals

having lower central frequencies will have a deeper zone of influence than signals having higher central frequencies.

There are two common collection modes for surface GPR data, and data from both of these modes can be used to calculate the groundwave velocity. The most frequently used mode is common-offset profiling, where the transmitting and receiving antennas are kept a fixed distance apart and are pulled in parallel along the ground surface. Common-offset profiling produces a series of measurements along a traverse. For the groundwave, the travel time and amplitude measurements recorded at each acquisition location are effective values over the sampling support area approximately represented by the antenna separation distance (S) and the depth of influence given in (1). The electromagnetic velocity of the groundwave for each common-offset acquisition location can be calculated by dividing the separation distance of the antennas by the measured travel time of the groundwave from the transmitter to the receiver. The other common collection mode for surface GPR data is variable-offset profiling, in which the separation distance between the transmitter and receiver is increased in even increments. For variable-offset data, the groundwave velocity is calculated by observing the changes in the groundwave arrival time as the antenna separation increases; the linear slope of travel time and antenna separation is the average velocity for the area between the two antennas. One form of variable-offset profiling is common-midpoint (CMP) surveys, in which the transmitter and receiver are each moved further apart by a constant increment for each new measurement. The other type of variable-offset profiling is wide-angle reflection and refraction (WARR) surveys, where one antenna is kept stationary while the other antenna is moved one distance increment for each new measurement. The sampling volume of variable offset data varies from the smallest value (when the antennas are closest together) to the largest value (when the antennas

are farthest apart), and the velocity measured with a variable offset survey is the effective velocity over the area between the smallest and largest antenna separations. The advantage of the variable-offset acquisition mode over the common-offset mode is that the data can be easily interpreted to provide quantitative velocity information about a single location. Although common-offset data require more complicated interpretation to extract quantitative velocity information, unlike variable-offset data, common-offset data can be collected quickly and easily over large areas.

Once the electromagnetic velocity (v) has been calculated, it can be converted to dielectric constant (κ) using an approximation appropriate for high radar frequencies in soils having low electrical conductivities (Davis and Annan, 1989):

$$\kappa \approx \left(\frac{c}{v}\right)^2, \tag{2}$$

where c is the speed of electromagnetic waves in a vacuum (3×10^8 m/s). For unsaturated soils, the dielectric constant is primarily dependent upon the water content of the soil, although other factors such as lithology, temperature, radar operating frequency, particle shape, and pore fluid composition may also contribute to the GPR response. The influence of water content on the dielectric constant of soil is caused by the large contrast in dielectric constant values between dry geologic materials (κ ~3-8), water (κ =81), and air (κ =1). Variations in the amount of water in the soil pores greatly change the dielectric constant of the soil, resulting in varying GPR travel times and amplitudes. Petrophysical models can be used to relate the dielectric constant to water content; these relationships can be developed for a specific soil or can be borrowed from literature. One of the most commonly used petrophysical relationships is an empirical

correlation developed by Topp et al. (1980) in the laboratory using TDR over a wide variety of agricultural soils:

$$\theta_v = -5.3\times10^{-2} + 2.92\times10^{-2}\kappa - 5.5\times10^{-4}\kappa^2 + 4.3\times10^{-6}\kappa^3, \quad (3)$$

where θ_V is volumetric water content. Other more mechanistic relationships have also been developed. For example, the complex refractive index method (CRIM) equation is a mixing model that relates the dielectric constant of the entire sample with the dielectric constants and volume fractions of different components of a soil (Wharton et al., 1980). While the CRIM model is often more accurate than Topp's equation, it requires knowledge of the porosity and the dielectric constant of the mineral grains, which are frequently unknown in field applications.

Many different approaches have been used to estimate volumetric water content using GPR data. Cross-borehole travel time measurements have recently been used in conjunction with petrophysical relationships to provide estimates of volumetric water content (Hubbard et al., 1997a, 1997b; Eppstein and Dougherty, 1998; Alumbaugh et al., 2000; Parkin et al., 2000; Binley et al., 2001). Cross-borehole GPR provides high-resolution information about the subsurface water content distribution, but this approach is invasive and requires sophisticated data processing. Other researchers have used GPR groundwave travel time data to estimate water content in the shallow subsurface. Du and Rummel (1994), van Overmeeren et al. (1997), and Huisman et al. (2001) used variable-offset data to estimate groundwave velocity. For variable-offset surveys, the estimated groundwave velocity data is used with (2) and a petrophysical relationship such as (3) to estimate water content. While variable-offset data can provide accurate estimates of water content, this collection mode is too time-consuming and labor-intensive to be useful for collecting many measurements in a practical field situation. Du and Rummel (1994) overcame this limitation by first collecting WARR data to identify the

groundwave and airwave arrivals, then collecting common-offset data. Comparison of the identified airwave and groundwave arrivals on WARR data with co-located common-offset data enabled identification of the groundwave and airwave on the common-offset data. They then used the common-offset data to estimate the water content along a traverse by measuring the travel time of the groundwave between the transmitting and receiving antennas and using the known antenna separation to calculate velocity. Although they did not verify their volumetric water content estimates, they observed that common-offset GPR measurements showed lower water content values in coarse-grained soils than in clayey soils. Lesmes et al. (1999) followed this approach to estimate water content in a 17 m^2 area over a three-week time interval using a grid of low-frequency (100 MHz) common-offset GPR groundwave data and compared the resulting GPR estimates of water content to measurements of water content obtained using TDR and gravimetric sampling. They found that the GPR estimates followed the same trends as the conventional measurements, but the absolute values of water content were significantly less than those found with conventional methods, possibly due to different sampling depths for low frequency GPR and conventional techniques. Huisman et al. (2001) collected higher frequency (225 MHz and 450 MHz) WARR groundwave data, TDR, and gravimetric measurements over 24 5-m traverses and found that the WARR groundwave velocities produced estimates of water content that agreed well with both the TDR and gravimetric water content measurements.

In addition to measurements of groundwave velocity to estimate water content, groundwave amplitudes may also hold information about soil moisture. Under conditions amenable to GPR data collection, GPR amplitudes decrease with increasing electrical conductivity and with increasing electromagnetic velocity (Davis and Annan, 1989). The electrical conductivity is a function of porosity, water content, and pore fluid conductivity and is

positively related to each of these parameters (Archie, 1942), while velocity is negatively related to water content, as discussed previously. In addition to the influences of conductivity and velocity, GPR groundwave amplitudes recorded at the receiving antenna may be affected by a variety of other factors, including the magnitude of the amplitude at the transmitter, separation distance between the transmitting and receiving antennas, ground cover, surface coupling, and scattering of the electromagnetic signal. Under some conditions, the amplitude may also be influenced by partial superposition of the airwave and groundwave. For example, the groundwave has an earlier arrival time in dry soils, and the groundwave signal may constructively superimpose with the airwave signal at small offsets to cause an increase in amplitude in dryer soils. When the soil is slightly wetter, the groundwave arrives later in time and has little or no superposition with the airwave. Although the numerous factors affecting groundwave amplitudes make theoretical calculations based on amplitude difficult, groundwave amplitude information may still be useful under controlled field conditions. For example, Chanzy et al. (1996) used the amplitude of common-offset groundwave ringing (repeated signals that mimic the real groundwave signal but occur later in time and that are caused by coupling between the ground and the GPR antennas) to empirically relate water content and amplitude at four small study sites. They observed a high degree of correlation between these parameters, and amplitude was shown to decrease with increasing water content.

The previous studies have shown that GPR groundwaves can be used both qualitatively and quantitatively for water content estimation. This experiment expands upon these results by testing the utility of GPR as a field tool for rapidly and accurately providing high-resolution estimates of volumetric water content under naturally heterogeneous conditions. Specifically, we investigate the use of high-frequency common-offset GPR groundwaves for obtaining

densely spaced estimates of water content over a large-scale agricultural field as a function of space and time. In addition to investigating spatial and temporal variations in water content and their relationship to precipitation and irrigation, we compare our volumetric water content estimates with gravimetric water content, TDR, and soil texture measurements and also consider information available from both GPR travel time and amplitude. Complementary to the groundwave analysis, we are also using reflections from natural soil layer interfaces to estimate water content associated with deeper soil zones, but this application is still in progress and will not be discussed herein.

3. Site Description and Data Acquisition

3.1. Site description

The study site is located next to the Robert Mondavi Winery near the town of Oakville in Napa County, California. The study site is approximately 10,000 m^2 and is planted with grapevines having row and vine spacing of 1.2 m each. The soils in the study area are generally described as belonging to the Bale series of the USDA Soil Conservation Service Classification System, which are somewhat poorly drained soils deposited in alluvial fan, flood plain, and low terrace settings and are derived from rhyolite and basic igneous rocks. The texture of the soil varies from sandy loam to clay loam, with the most common textures being sandy loam and sandy clay loam. Topographic variations across the study site are negligible, and the water table is approximately 4 m below ground surface. Summers are hot and dry; most precipitation occurs during the cool winters. The mean annual precipitation for this area is 0.64 to 0.89 m. Irrigation is performed uniformly across the site using a drip irrigation system during the driest months, from May/June to September/October, with an average irrigation rate of 0.014 m/week.

Remote sensing data were used as a factor in choosing the study site. Remote sensing data were acquired at the Mondavi site in August 1998, August 1999, and July 2000 using airborne ADAR Multispectral System 5500 (Positive Systems) collecting in the blue, green, red and near-infrared portions of the spectrum from a flight altitude of 4300 m above the ground surface and with a spatial resolution of 2m x 2m (Johnson et al., 2000). The frequencies used to collect the remote sensing data are higher than those used in the microwave systems typically employed to estimate soil water content in areas of sparse vegetation. These higher frequency data were processed to yield normalized different vegetation index (NDVI) data, which relate the proportions of photosynthetically absorbed radiation in the visible and near-infared wavelengths. NDVI data can be correlated to the density, or vigor, of vegetation. Variations in NDVI within an area often reflect differences in irrigation, nutrient availability, vineyard geometry, rootstock, and disease or pest infestation (Penn, 1999; Carothers, 2000). The site map shown in Figure 1 is superimposed on NDVI imagery collected in July 2000; in this image the darker areas are indicative of weak vegetation, and the lighter zones signify more vigorous vegetation. The NDVI images from the three data sets collected at this site are all very similar, suggesting that the same factors influence vegetation vigor each year. At this site, all agricultural parameters (vine and row spacing, trellis type, and rootstock) and practices (irrigation, fertilization, and pruning) are constant throughout the vineyard, and variations in topography are minimal. The uniformity of these parameters suggests that the variations in vegetation vigor shown by the NDVI data may be a function of soil texture and moisture availability. The variability displayed in the NDVI data was one of the factors used in selection of the field site, since a site with significant soil heterogeneity was desired for this GPR investigation.

3.2. Data acquisition

Several different types of data were collected at the study site, including surface GPR, cross-borehole GPR, gravimetric water content, TDR, neutron probe, and soil texture data. Figure 1 shows the site geometry and the location of many of these measurements. Surface GPR data were collected using a Sensors and Software PulseEkko1000 system at central frequencies of 450 MHz and 900 MHz, with bandwidths approximately equal to the central frequency. Very high-resolution surface GPR data were collected over selected 1 m Dense Sampling Areas (DSAs) throughout the field in September 2001, November 2001, and January 2002, as shown on Figure 1. Very high-resolution data were collected at the DSAs to develop groundwave interpretation techniques and to compare the accuracy of the water content estimates obtained from GPR data with co-located point measurements obtained from conventional methods, as will be discussed in Section 4. GPR data were collected at the DSAs using both frequencies; common-offset data were acquired using 2 cm increments, and CMPs were collected using antenna separations that increased by 2 cm for each measurement to a final antenna separation of 1 m.

In addition to the DSA GPR data, we also collected several full-field grids of GPR data over the entire field site shown in Figure 1. Grids of common-offset GPR data were collected across the site by taking measurements at least every fifth row between rows 35 and 155 (Figure 1), with a sampling interval of 10 cm within each row. Data were collected over the entire field grid over a nine-month period during four field campaigns; the campaigns occurred in May 2001, August 2001, September 2001, and January 2002. The data campaigns were scheduled to capture the major seasonal variations in water content at the site. The May campaign occurred after the rainy season but before irrigation, the August and September data were collected during the hot, dry summer and during irrigation, and the January campaign was performed during the

rainy season. Interpretation of the grid data following the procedure developed in the DSAs will be discussed in Section 5.

For both the full-field grid data and the data collected at the DSAs, the sampling intervals of the 900 MHz and 450 MHz data were 100 and 200 picoseconds, respectively. Data were collected (stacked) 16 to 32 times at each acquisition station to enhance the recorded GPR signal over random noise contributions. Data processing for travel time information was minimal and included bandpass filtering to remove low-frequency induction effects and amplitude balancing down each trace. For amplitude processing of common-offset data, only the bandpass filter was applied.

Cross-borehole GPR measurements were taken between several of the five boreholes shown in Figure 1 to a depth of 4 m. One set of boreholes is located in the most clay-rich area of the site, while the other set of boreholes is located within a sandier area. Cross-borehole GPR data were taken with a Sensors and Software PulseEkko100 system using a central frequency of 200 MHz. Measurements were taken in a zero-offset mode to provide a vertical profile of average electromagnetic velocity between borehole pairs, as described by Peterson (2001).

Gravimetric water content, TDR, soil texture, and neutron probe measurements were acquired using standard data collection and interpretation techniques, such as are described in Haverkamp et al. (1999). The average sample volume for both the gravimetric water content and textural analyses was 250 cm^3, and over 150 of these co-located measurements were collected from both near-surface soil samples and from samples taken at 30 cm intervals in the boreholes shown in Figure 1 from the ground surface to the water table. The near-surface samples were usually collected in pairs, with one sample taken over the interval from 0-10 cm and the second sample taken over 10-20 cm depth. Each soil sample was divided into two portions; gravimetric

water content was measured using one portion, and the soil texture (percent sand, silt, and clay of the non-gravel component) was measured on the other. TDR data were collected using a SoilMoisture Trase System with two 15 cm waveguides placed 5 cm apart and a central frequency of approximately 3 GHz. The average sample volume of a TDR measurement was a cylinder of approximately 750 cm^3 centered around the waveguides. The near-surface gravimetric water content, soil texture, and TDR measurements were taken coincident with the GPR data within the DSAs; these point measurements were taken at the center of each 1-m traverse for calibration and validation of the GPR data. Neutron probe measurements were taken in each of the 16 boreholes shown in Figure 1 using a CPN 503DR Hydroprobe with a vertical sampling interval of 7.5 to 15 cm. The neutron probe measurements, collected immediately after borehole construction, were used in conjunction with co-located gravimetric water content measurements taken on the samples retrieved from the same boreholes to develop a site-specific petrophysical relationship between backscattered neutron counts and gravimetric water content. The petrophysical relationship was developed using linear regression and suggested that the correspondence between the neutron counts and gravimetric water content measurements was reasonable ($R = 0.84$) and that the neutron probe measurements were not sensitive to soil texture. By assuming a soil density of 1.65 g/cc and a water density of 1.00 g/cc, we converted the gravimetric water content measurements into volumetric water content estimates for comparison of the neutron probe data with electromagnetic velocities measured between the boreholes using cross-borehole GPR.

4. Data Interpretation and Correlations using Detailed Study Area (DSA) data

In this section, we discuss the development and validation of the methodology used to estimate volumetric water content from GPR groundwave data using data collected in the DSAs.

This analysis includes estimation of groundwave velocities using common-offset GPR data, determination of an appropriate petrophysical relationship, and validation of our interpretation method for GPR groundwave estimation of water content. We also discuss the correlations between different types of data collected within the DSAs, including estimates of water content from TDR and GPR travel times, water content and GPR groundwave amplitudes, and water content and soil texture.

4.1. Estimation of groundwave velocity

Before groundwave velocity can be estimated, the airwave and groundwave signals must be correctly identified on the GPR data. A straightforward technique for identifying airwave and groundwave signals on common-offset GPR data is given in Du and Rummel (1994). With this technique, co-located common-offset and variable-offset surveys are collected. The airwave and groundwave can be easily identified on the variable-offset survey, since each wave has a distinct slope (time vs. distance). Once the airwave and groundwave are identified on the variable-offset data, the pattern of amplitude and travel time created by these waves is determined at the antenna separation used to collect the common-offset surveys. The common-offset data are then analyzed to identify the same pattern of amplitude and travel time at times near the expected arrival time of the airwave and groundwave, where the expected arrival time is based on the average electromagnetic velocity of the soil and the known antenna separation. By matching the patterns generated by the airwave and groundwave in the variable-offset survey with those in the corresponding common-offset surveys, the airwave and groundwave can be chosen without ambiguity on the common-offset data. The common-offset data can then be used to quickly collect groundwave information over large areas. An example of an interpreted 450 MHz common-offset profile along a 1 m traverse is shown in Figure 2. In this figure, each trace, or

vertical line, exhibits the airwave and groundwave signals recorded at a single surface location. The horizontal axis shows the location along the traverse of each measurement, and the vertical axis is the travel time of the electromagnetic energy. The airwave has a faster velocity than the groundwave, and thus the airwave arrives at an earlier travel time. The airwave and groundwave 'picks' were chosen based upon the arrival times of these waves in co-located CMP data at 25 cm offset, which corresponds to the separation distance of the transmitting and receiving antennas (S) in the common-offset data. The difference in arrival times between the airwave and groundwave (Δt in Figure 2) was calculated at each point along the traverse. The airwave does not mark the onset time of the signal, but instead provides a clear and 'pickable' event. As the signal onset occurs at a time prior to the arrival of the airwave, a constant value was added to each Δt to account for the onset delay time represented by the time required for the signal to travel in air the distance (S) between the transmitter and the receiver. The final groundwave travel time (t_T) is given by

$$t_T = \Delta t + \frac{S}{c}, \tag{4}$$

where c is the speed of electromagnetic waves in air. For each location, once the groundwave travel time was found, the velocity was calculated using the common-offset antenna separation, and the velocity was converted to dielectric constant using (2).

4.2. Development of petrophysical relationships

To estimate volumetric water content from dielectric constant values, a petrophysical relationship such as (3) must be invoked. We developed two site-specific petrophysical relationships, one using near-surface measurements collected within the DSAs, and the other using cross-borehole GPR measurements. The relationship developed from near-surface

measurements uses co-located dielectric constant values from TDR and volumetric water content values from gravimetric water content measurements collected in the DSAs. This relationship was developed using heterogeneous soil samples, covers the range of water content that we are investigating with GPR groundwave techniques, and has a sampling volume similar to that of the GPR groundwaves. The cross-borehole GPR relationship was developed using co-located, zero-offset cross-borehole radar data (interpreted in terms of dielectric constant) collected over a scale of 2-4 m and neutron probe backscatter counts (interpreted in terms of volumetric water content) collected from borehole pairs at the two locations shown in Figure 1. The cross-borehole relationship was developed using soils that were deeper and wetter than most of the near-surface soils sampled by TDR and by GPR groundwaves, so the range of water contents where this relationship is applicable is somewhat different than for the TDR-based relationship. One cause for error in both of the site-specific relationships is that a constant density was used to convert the gravimetric water content measurements to volumetric water content estimates, and the true density is probably slightly different for each measurement. Despite this error, both site-specific relationships are similar to the widely used Topp's equation (3), as is shown in Figure 3. The differences between the site-specific relationships are most likely due to the differing ranges of water content used to develop the relationships and to the uncertainty in the cross-borehole relationship produced by the differences in sample volume between the cross-borehole dielectric constant measurements and the neutron probe estimates of water content.

Since the TDR-based relationship covers a similar range of water content as that measured with GPR groundwaves and has less uncertainty than the cross-borehole relationship, the TDR-based relationship was preferred over the cross-borehole relationship to convert GPR groundwave estimates of dielectric constant to water content. However, before applying the

TDR-based relationship to GPR groundwave data, the differences in the sample volumes and frequencies of the TDR and GPR must be considered. Huisman et al. (2001) addressed these issues and showed that large-scale (up to 5 m antenna separation) GPR groundwave measurements and co-located gravimetric measurements produced empirical petrophysical relationships very similar to those obtained with small-scale TDR and gravimetric water content measurements for a variety of soils. From these results, Huisman et al. concluded that relationships developed using TDR could be applied to GPR groundwave data. Other researchers have considered similar issues; White and Zegelin (1995) showed that dielectric constant (used to estimate water content) was independent of frequency in the ranges used by both the GPR and TDR in this study. These results are in conformity with those of other researchers (Du and Rummel, 1994; Greaves et al., 1996; Hubbard et al., 1997a; Grote et al., 2002) who have successfully applied petrophysical relationships developed at the laboratory scale using TDR on larger-scale measurements of dielectric constant from GPR to obtain estimates of water content. Based upon these findings, the similar water content ranges and sample sizes measured by the TDR and GPR groundwaves, and the excellent correlation between dielectric constant from TDR and volumetric water content (R = 0.95), it was determined that the TDR-based relationship developed at this site was applicable to GPR groundwave measurements of dielectric constant.

4.3. Validation of water content estimation procedure using GPR groundwaves

We tested the accuracy of the data interpretation procedure and the TDR-based petrophysical relationship described in Sections 4.1 and 4.2 on surface GPR data collected within the 1-m long DSAs shown in Figure 1. Estimates of volumetric water content obtained from GPR groundwaves were compared to co-located estimates of volumetric water content from gravimetric samples obtained from 0-20 cm depth in the middle of each GPR traverse, as

described in Section 3. Below, we discuss these comparisons for both CMP and common-offset GPR data.

CMP surveys were used to estimate the groundwave velocity at each DSA, and the velocity was converted to dielectric constant and then to water content using the relationship described in Section 4.2. As shown in Table 1, comparison of the volumetric water content estimates derived from CMP data and from gravimetric measurements showed a very good linear correlation for the 900 MHz data and a decent linear correlation for the 450 MHz data. Some of the error in the CMP estimates could be due to the different sampling volumes of the GPR signals and the gravimetric measurements or to inaccuracies in determining the CMP velocity when partial airwave and groundwave superposition occurs at small antenna offsets. The 450 MHz data has a longer wavelength and therefore experiences more airwave and groundwave superposition at small offsets than does the 900 MHz data, so the 450 MHz data may be more prone to errors in velocity estimation when the antennas are very close together. Despite the possible reasons for error, the correlations from both frequencies show that CMP velocities were sensitive to water content at this site. Although these results suggest that CMP data can be used successfully for water content estimation, CMP surveys are time consuming to collect and interpret and so are not practical for field monitoring. Common offset data, which can be collected and interpreted quickly, are preferable for large-scale monitoring of water content.

Common-offset data were acquired at 2 cm increments (as shown by Figure 2), and the t_T values for each trace (4) were averaged over the 1 m traverse to provide a single volumetric water content estimate from common-offset GPR for each DSA. This averaging also helped to reduce error due to imprecise location coordinates and to compensate for measurement error in individual GPR traces. These averages were then converted to water content estimates as

described in Sections 4.1 and 4.2 and were compared to the water content values obtained from gravimetric sampling. Figure 4 shows these comparisons, and the results are also listed in Table 1. Both the 900 MHz and 450 MHz common-offset estimates correlate well with the water content from gravimetric sampling, with linear correlation coefficients (R) of 0.95 and 0.97, respectively. As was also observed with the CMP data, common-offset GPR data from both frequencies yield volumetric water content estimates that were on average slightly higher (~0.017) than the gravimetrically obtained estimates. The apparent overestimation of water content from GPR data may be due to underestimation of the soil density used to convert gravimetric water content measurements to volumetric water content estimates or to water loss in the gravimetric samples between collection and processing.

The common-offset travel time data were also useful for investigating the depth of influence of the groundwaves. Using the central frequencies observed in the data spectra (somewhat lower than the central frequencies of the antennas), the average groundwave velocity from CMPs, and the measured antenna separation distance, the zone of influence calculated using (1) extends from the surface to approximately 7 cm in wetter soils and 10 cm in dryer soils for the 900 MHz data and 11 cm in wetter soils and 14 cm in dryer soils for the 450 MHz data. These theoretical zones of influence were compared to near-surface gravimetric measurements sampled over depths of 0-10 cm and 10-20 cm and averaged over 0-20 cm. Both the 900 MHz and the 450 MHz data show the highest correlation with the gravimetric water content averaged over 0-20 cm and the least correlation with the water content in the 10-20 cm interval. These correlations imply that the depth of influence for this data set may be slightly deeper than that predicted using (1), but that the predictions are reasonable. Differences in the water content estimates from the 900 MHz and 450 MHz data are also indicative of the depth of influence.

One DSA campaign (November) was performed one day after a light rainfall, and the gravimetric water content samples showed that the soil in the 0-10 cm zone was wetter than that in the 10-20 cm zone. The common-offset GPR data collected at this time showed that the 900 MHz data produced higher estimates of water content than the corresponding 450 MHz estimates. Although these studies show that the 450 MHz data has a deeper zone of influence than the 900 MHz data, gravimetric measurements taken at smaller vertical intervals during times of known vertical heterogeneity are necessary to more accurately establish the depth of influence of each frequency.

4.4. Correlation of water content estimates from GPR groundwaves and TDR

TDR measurements were collected at the center of each 1 m DSA, and comparisons were made between volumetric water content estimates obtained from TDR and coincident GPR common-offset data averaged over the 1 m traverse. These analyses showed that TDR and GPR estimates of water content gave similar values and had approximately the same error, despite differences in measurement technique and sample volume. The root mean squared error (RMSE) of volumetric water content from TDR when compared to the volumetric water content sampled gravimetrically over 0-20 cm was 0.020, and the RMSE from the 900 MHz and 450 MHz GPR data were 0.025 and 0.026, respectively. The excellent correlations between the water contents estimated using TDR and GPR data is given in Table 1. The slightly higher correlation between the TDR and 450 MHz data shown in Table 1 is likely due to the more similar sampling depth of the TDR (~15 cm) and the 450 MHz groundwaves (~11-14 cm).

4.5. Correlation of water content and GPR groundwave amplitudes

As described in Section 2, although the contributions from the different factors affecting GPR groundwave amplitude measurements are difficult to quantify, empirical relationships

between amplitude and water content may be useful. To investigate the empirical relationship between groundwave amplitude and water content at this site, common-offset amplitudes were compared to gravimetric water content measurements collected in the DSAs. Amplitude analysis consisted of finding the maximum and average of the absolute values of amplitude over a time window on the GPR signal in which the groundwave was the dominant event; Figure 2 shows an example of a groundwave-dominated time window along a DSA traverse. In this figure, the higher amplitudes are indicated by either the positive (black) or negative deviations of the signal from a vertical baseline. By averaging the absolute values of groundwave amplitude within a time window (such as that shown in Figure 2) along each DSA traverse, reasonable correlations were found between amplitude and gravimetric water content. The main advantage of using empirical amplitude data over travel time data for estimating water content is that the exact identification of the airwave and groundwave is less important. This reduces the number of points that need to be picked (uses a window of data rather than the exact arrival time of the airwave and groundwave) and facilitates faster data interpretation, which lessens the time required for data processing. Additionally, fewer CMPs are needed to verify common-offset amplitude measurements, so data collection may also be faster

Examples of the correlations between average 900 MHz and 450 MHz groundwave amplitudes and gravimetrically obtained measurements of volumetric water content collected in the DSAs in September 2001 are shown in Figure 5. Data collected at other times also showed that measured amplitudes from both frequencies decrease with increasing water content, but the correlations between amplitude and water content were slightly different at each time. These differences are likely caused by variations in ground cover and by partial airwave and groundwave superposition. The 900 MHz amplitude data usually have better correlations with

water content than the 450 MHz data, probably because the 900 MHz signal has a smaller wavelength and therefore less airwave and groundwave superposition. Although more research is necessary to quantitatively extract reliable information from common-offset amplitudes, these correlations indicate that empirical amplitude analysis of common-offset GPR data may give a reasonable indication of volumetric water content.

4.6. Correlation of water content and soil texture

Soil texture, as quantified by percent sand, silt, and clay, was measured coincidently with gravimetric water content during data collection at the DSAs, as described in Section 3. Figure 6 shows the correlations between percent sand and gravimetrically derived volumetric water content for each of the DSA data acquisition campaigns. This plot shows that there is a consistent correlation of decreasing water content with increasing percent sand, and that these correlations have a temporal component. This result is expected, as the soils with lower sand content (and thus higher fractions of silt and clay) will drain less easily and have a higher average water content.

5. Estimation of spatial and temporal variations in water content using GPR grid data

The interpretation techniques developed in the detailed studies discussed in Section 4 were applied to the full-field grids of GPR data to assess near-surface variations in volumetric water content over space and time. Full-field GPR data were collected at 900 MHz and 450 MHz along every fifth row as described in Section 3, and the travel time data were analyzed and converted to water content as described in Section 4. Empirical relationships between average amplitude and volumetric water content, as described in Section 4.5, were developed and applied to selected full-field GPR data grids. The following discussion focuses on the full-field water

content distributions with time, space, and depth as determined from the GPR travel time and amplitude data and comparison of the water content distributions with full-field soil texture data.

5.1. Estimation of water content using GPR travel time data

The water contents calculated from 900 MHz groundwave travel time data for each full-field data campaign and the corresponding average water content (θ_V) calculated from these estimates are shown in Figure 7. These data grids have been smoothed to show the significant trends in water content (rather than the exact value of each of the approximately 20,000 points in every grid) by averaging each point by the surrounding eight points. The resulting spatial patterns of water content are similar for all surveys, even though the average water content fluctuates seasonally. Note that Figures 7a, 7b, and 7c have the same water content range (0.1 to 0.2), while the range in Figure 7d is considerably higher (0.25 to 0.35); the change in scales is necessary to show local variations in water content. As will be discussed in Section 5.3, we interpret that the persistent spatial pattern seen in each of these figures is controlled by soil texture.

The average water content from each GPR survey shows the effects of seasonal precipitation and irrigation. The May survey occurred at the beginning of the dry season, one week after a light precipitation event, while the August survey was taken during the dry season, three weeks after the most recent irrigation. The September data were also collected during the dry season, but only two days after irrigation, and the January data were taken one day after light precipitation during the rainy season.

The 450 MHz travel time data were also analyzed and converted to water content. The spatial distribution of water content from the 450 MHz data is similar, but not identical, to that observed on the 900 MHz data, and the average water content values obtained from the 450 MHz

grids are usually a few percent higher than the corresponding values obtained from the 900 MHz grids. Figure 8 shows the water content estimates from the 450 MHz travel time data during a relatively dry time (September) and during a wetter time (January). (Again note that the range of water content for the January data is higher than that of the September data.) Comparison of Figures 8a and 8b with Figures 7c and 7d, respectively, shows that the spatial distribution associated with the 450 MHz data is similar to that seen with the 900 MHz data. The differences in spatial pattern and average water content between the 900 MHz and 450 MHz grids are probably caused by the deeper sampling zone of the 450 MHz data. In the absence of recent infiltration, the soil nearest the surface is usually dryer than the deeper soils, and thus the 900 MHz data would sample a dryer soil zone than the 450 MHz. This is the case for the data collected in August, where the average water content of the 450 MHz data is 0.06 higher than that of the 900 MHz data. However, for the January field grids, which were collected one day after a precipitation event, the 900 MHz and 450 MHz data show the same average water content, implying that the soil was either uniformly saturated or that the sampling zones of the two frequencies are more similar in wetter soils.

5.2. Estimation of water content using GPR amplitude data

As described in Section 4.5, although GPR groundwave amplitudes currently can only be empirically correlated to water content, amplitude data may provide reasonable indications of the moisture content distribution and can be collected and processed more quickly than travel time data. For this experiment, amplitude analysis was conducted on full-field common-offset grids that coincided with the collection of a significant number of gravimetric water content measurements. Amplitude analysis consisted of calculating the average of the absolute values of amplitude in a groundwave-dominated time window for each GPR measurement, as described in

Section 4.5. Analysis of co-located average amplitude and gravimetric water content measurements permitted development of an empirical amplitude-water content relationship for each grid. The full-field grids of amplitude were then converted to water content using the time-dependent relationship appropriate for each survey. Figures 9a and 9b show the full-field grids of water content estimated using the groundwave amplitude data collected at both 900 MHz and 450 MHz during the September survey, together with the empirical relationships for this data set (shown in Figure 5). Comparison of Figure 9a and 7c and comparison of Figure 9b and 8a show that the spatial patterns and the average water content values derived from amplitudes are similar to those derived from travel time data, although some variations in the two techniques are evident. A more rigorous analysis of GPR amplitudes is ongoing and may ultimately provide an approach for estimating both water content and soil texture from joint travel time and amplitude GPR data.

5.3. Comparison of GPR-estimated water content and soil texture

The correlation of water content and percent sand observed in the DSAs (Section 4.6) implies that the spatial distribution of water content estimated using GPR data could be used to indicate the soil texture in the near surface. A contour plot of the soil texture in the interval from the ground surface to a maximum of 30 cm deep, as derived from measurements collected during near-surface studies and from the uppermost borehole samples, is shown in Figure 10. The textures in this plot are expressed as percent sand, where the remaining soil is composed of the silt and clay components. The spatial pattern illustrated in Figure 10 is very similar to the GPR-derived water content patterns (for example, Figure 7). Areas of high percent sand correspond to the areas that are consistently dryer on the GPR-obtained water content maps, and the zones with low percent sand are consistently wetter. While this result may be useful for estimation of

shallow soil textures, the relationship is probably not valid for deeper soils because infiltration and drainage are more time and depth dependent in deeper soils.

6. Summary

This experiment has shown that GPR groundwave data can be used as a field tool to accurately, non-invasively, and rapidly estimate shallow water content in a field scale application. Analysis of travel time data produces reliable results with a sampling density much greater than that available with conventional point measurement techniques. Empirical analysis suggests that calibrated amplitude data may also hold potential for a quick and simple method of water content estimation. Multi-frequency GPR data can be employed to determine both the lateral and vertical distribution of water content, as lower frequencies can estimate water content at greater depths than higher frequencies. Our results showed that water content at this field site is vertically heterogeneous in the zone between 9 and 15 cm below the ground surface, and 900 MHz and 450 MHz GPR data can capture this heterogeneity. The temporal persistence of the spatial distribution of water content as seen from both GPR frequencies and the similarity of this pattern to the soil texture distribution suggest that soil texture is a controlling factor on near surface soil water content at the Robert Mondavi Winery site.

The results from this experiment can be applied to improve agricultural practices. By estimating the soil water content before starting irrigation, the optimal scheduling and amount of irrigation can be determined, and irrigation can be applied non-uniformly across as field as needed. The GPR estimates of water content could also be used to indicate soil texture, so calibrated GPR measurements could be used to identify poor soil conditions and to optimize the planning of vineyard layout (geometry and plant density) and agricultural practices for new vineyards. GPR is a useful tool for these applications because the spatial density of conventional

point measurements of water content is typically insufficient to capture the complete pattern of soil moisture over a large area, and due to the variability of water content, a few point measurements may indicate an incorrect water content distribution.

We are continuing to develop and refine the use of GPR data for water content estimation in agricultural applications. One aspect of this process is to collect deeper information using reflections from natural soil layers in vineyards; this will allow analysis of the water content in the deeper root zone. Another aspect is to perform geostatistical analysis of the GPR groundwave data and the conventional point measurements to investigate the correlation structures of estimates obtained using the various techniques (Grote et al., 2001). We are also developing a more thorough method for amplitude analysis, including comparison of common-offset amplitudes with attenuation from CMPs and studying correlations between amplitude, water content, and soil texture. Finally, we are collecting resistivity data with co-located GPR measurements to create a more complete image of the water content distribution with depth.

The results presented in this study show that GPR groundwaves can be used as a field tool for estimating volumetric water content. To our knowledge, this is the first time that volumetric water content has been estimated with high resolution over a large-scale heterogeneous field site with measurements collected over both space and time. The detailed water content information collected using this method could be used as input to vadose zone and meteorological modeling, precision agriculture, and water resources management.

Acknowledgements

This study was funded by USDA 2001-35102-09866, NSF EAR-0087802, and WRC project W-929 to Yoram Rubin. We sincerely thank Daniel Bosch and the Robert Mondavi Winery for providing vineyard access and technical information. We also thank Lee Johnson (CSU

Monterey Bay and NASA/Ames Research Center) for providing access to the remote sensing imagery.

References

Alumbaugh, D., L. Paprocki, L. Brainard, and C. Rautman, Monitoring infiltration within the vadose zone using cross-borehole ground penetrating radar", In: Proc. Symp. Applications of Geophysics to Engineering and Environmental Problems (SAGEEP), Environmental and Engineering Geophysical Society, 273-281, 2000.

Archie, G.E., The electrical resistivity log as an aid in determining some reservoir characteristics,

Trans. Am. Inst. Mining Met. Eng., 146, 54-62, 1942.

Berktold, A., K.G. Wollny, and H. Alstetter, Subsurface moisture determination with the ground wave of GPR, *Proc., GPR 98 Conference*, 1998.

Binley, A.P., R Winship, M. Middleton, M. Pokar, and J. West, High resolution characterization of vadose zone dynamics using cross-borehole radar, *Water Resour. Res.*, 37(11), 2639-2652, 2001.

Carothers, J., Imagery technology meets vineyard management, *Practical Winery and Vineyard*, May 2000.

Chanzy, A., A. Tarussov, A. Judge, and F. Bonn, Soil water content determination using digital ground-penetrating radar, *Soil Science of America Journal* 60, 1318-1326, 1996.

Davis, J.L. and A.P. Annan, Ground penetrating radar for high-resolution mapping of soil and rock stratigraphy, *Geophysical Prosp.*, 37, 531-551, 1989.

Du, S. and Rummel, P. Reconnaissance studies of moisture in the subsurface with GPR, Proc. Int. Conf. Ground Penetrating Radar 5th, Kitchener, Ontario, Canada, Vol.3, Waterloo Centre for Groundwater Res., Univ. of Waterloo, ON. 1241-1248, 1994.

Eppstein, M.J. and D.E. Dougherty, Efficient three-dimensional data inversion: Soil

characterization and moisture monitoring from cross-well ground-penetrating radar at the Vermont test site*, Water Resour. Res.*, 34(8), 1889-1990, 1998.

Frolich, R. K., and C. D. Parke, The electrical resistivity of the vadose zone – Field Survey, *Ground Water* 27(4), 424-530, 1989.

Greaves, R.J., D.P. Lesmes, J.M. Lee, and M.N. Toksoz, Velocity variations and water content estimated from multi-offset ground penetrating radar, *Geophysics* 61, 683-695, 1996.

Grote, K., S. Hubbard, and Y .Rubin, Soil Water Content Spatial Correlation Estimation using GPR, *EOS Trans. AGU*, 82(47), Fall Meet. Suppl., H31C-0247, 2001.

Grote, K., S. Hubbard, and Y. Rubin, GPR monitoring of volumetric water content in soils applied to highway construction and maintenance, Leading Edge, 482-285, 2002.

Hagedoorn, J., A process of seismic reflection interpretation, *Geophys. Prosp*., 2, 85-127, 1954.

Haverkamp, R., F. Bouraoui, C. Zammit, and R. Angulo-Jaramillo, Soil properties and moisture movement in the unsaturated zone, Chapter 5 in *The Handbook of Groundwater Engineering*, J. Delleur (Ed.), CRC Press, NY, 1998.

Hubbard, S., J.E. Peterson, E.L. Majer, P.T. Zawislanki, K.H. Williams, J. Roberts, and F. Wobber, Estimation of permeable pathways and water content using tomographic radar data, *Leading Edge*, 1623-1628, 1997a.

Hubbard, S.S., Y., Rubin, and E. Maher, Ground penetrating radar for saturation and permeability estimation in bimodal systems, *Water Resour. Res.,* 33( ), 971-990, 1997b.

Huisman, J.A., C. Sperl, W. Bouten, J.M. Berstraten, Soil water content measurements at different scales: accuracy of time domain reflectometry and ground penetrating radar, *Journal of Hydrology*, 245, 48-48, 2001.

Jackson, T.J., J. Schmugge, and E.T. Engman, Remote sensing applications to hydrology: soil moisture, *Hydrological Sciences*, 41(4), 517-530, 1996.

Johnson, L., R. Nemani, L. Pierce, M. Bobo, and D. Bosch, Toward the improved use of remote sensing and process modeling in California's premium wine industry*, Proc. IEEE International Geoscience and Remote Sensing Symposium*, Vol. 1, 363-365, 2000.

Kean, W. F., M. J. Waller, and H. R. Layson, Monitoring moisture migration in the vadose zone with resistivity, *Ground Water*, 25(5), 562-571, 1987.

Lesmes, D., R.J. Herbstzuber, and D. Wertz, 1999, Terrain permittivity mapping: GPR measurements of near-surface soil moisture, Proc. Symp. Applications of Geophysics to Engineering and Environmental Problems, Environmental and Engineering Geophysical Society, 575-582, 1999.

Luck, E. and M. Eisenreich, Electrical conductivity mapping for precision agriculture, Proc., Third European Conference on Precision Agriculture, France, 425-429, June 2001.

Mancini, M., R. Hoeben, and P. A. Troch, Multifrequency radar observations of bare surface soil moisture content: A laboratory experiment, *Water Resour. Res.,* 35(6), 1827-1838, 1999.

Mauser, W., M. Rombach, H. Bach, A. Demircan, and J. Kellndorfer, Determination of spatial and temporal soil-moisture development using multitemporal ERS-1 data, Proceedings, Multispectral and Microwave Sensing of Forestry, Hydrology, and Natural Resources, SPIE, Vol. 2314, 502-515, 1994.

Parkin, D., P. Redman, P. von Bertoldi, and Z. Zhang, Measurement of soil water content below a waterwater trench using ground penetrating radar, *Water Resour. Res.*, 36(8), 2147-2154, 2000.

Penn, C., Grape growers gravitating toward space age technologies, *Wine Business Monthly*, 53-56, Feb. 1999.

Peterson, J., Pre-inversion corrections and analysis of radar tomographic data, *Journal of Environmental and Engineering Geophysics*, 6(1), 1-18, 2001.

Prichard, T., Soil moisture measurement technology, Wine Grape Irrigation Short Course, University of California at Davis Extension, 1999.

Pultz, T. J., R. LeConte, J. Brown, and B Brosco, Quantitative soil moisture extraction from airborne SAR data, *Can. J. Remote Sens*. 16, 56-62, 1990.

Sheets, K.R. and J.M.H. Hendrickx, Non-invasive soil water content measurement using electromagnetic induction, *Water Resour. Res.,* 31(10), 2401-2409, 1995.

Topp, G.C., J.L. Davis, and A.P. Annan, Electromagnetic determination of soil water content: measurements in coaxial transmission lines, *Water Resour. Res.,* 16(3), 574-582, 1980.

Van Overmeeren, R., Sariowan, S., and Gehrels, J., Ground penetrating radar for determining volumetric soil water content; results of comparative measurements at two test sites, *Journal of Hydrology* 197, 316-338, 1997.

Western, A.W., G. Blöschl, and R. B. Grayson, Geostatistical characterization of soil moisture patterns in the Tarrawara catchment, *J. Hydrol., 205*, 20-37, 1998.

Wharton, R.P., G.A. Hazen, R.N. Rau, and D.L. Best, Advancements in electromagnetic propagation logging, *Soc. Petr. Eng*., Paper 9041, 1980.

White, I. and S.J. Zegelin, Electric and dielectric methods for monitoring soil-water content,

Chapter 22 in *Handbook of vadose zone characterization and monitoring*, L.G. Wilson, L.G. Everett, and S. Cullen (Eds.), Lewis Publ., Ann Arbor, MI, 1995.

Williams, L.E., N.K. Dokoozlian, and R. Wample, *Handbook of Environmental Physiology of Fruit Crops, Vol. 1: Temperate Crops*, *Chpt. 4*, B. Schaffer and P.C. Anderson (Eds.), CRC Press, Boca Raton, 1994.

Figure Captions

Figure 1 Site map showing the positions of the dense sampling areas (DSAs), neutron probe boreholes, and cross-borehole radar measurements superimposed on NDVI imagery acquired during July 2000. The x-axis on this map is the number of the vineyard row, and the y-axis is the vine number.

Figure 2 Interpreted 450 MHz GPR common-offset traverse. The x-axis is distance along the traverse, and the y-axis is the travel time of the GPR signal. The amplitude is represented by variations from a vertical baseline of the GPR signal with time.

Figure 3 Comparison of two site-specific petrophysical relationships with an empirical relationship often used in agricultural applications (3). Solid lines are used to designate the ranges of water content and dielectric constant where data that were used to develop each of the site-specific relationships were collected, and dashed lines are used to show where the site-specific relationships have been extrapolated beyond the ranges of the data that were actually collected.

Figure 4 Comparison of volumetric water content estimates derived from common-offset 900 MHz and 450 MHz GPR data collected at DSAs with coincident volumetric water content measurements obtained gravimetrically. These correlations show that common-offset groundwave data can be used to accurately estimate volumetric water content, although some bias is evident in this data.

Figure 5 Correlation of average amplitudes from 900 MHz and 450 MHz common-offset data collected at DSAs in Sept. 2001 with coincident volumetric water content measurements obtained gravimetrically. These correlations suggest that GPR groundwave amplitude data may be useful for water content estimation.

Figure 6 Comparison of shallow soil texture, quantified as percent sand, with volumetric water content derived from gravimetric sampling during the detailed studies.

Figure 7 Comparison of the volumetric water content distribution estimated using 900 MHz common-offset travel time data over the entire field at four times throughout a nine month period. Note that the range of water content in 7d is higher than at other times. These plots show that the spatial pattern of water content at this site does not change with time, although the absolute water content values fluctuate seasonally.

Figure 8 Comparison of the volumetric water content distribution estimated using 450 MHz common-offset travel time data over the entire field during two data campaigns. The spatial pattern observed in the 450 MHz data is similar, but not identical, to that seen in the 900 MHz data.

Figure 9 Comparison of the volumetric water content distribution estimated using 900 MHz (9a) and 450 MHz (9b) common-offset amplitude data over the entire field in Sept. 2001. The spatial patterns produced by these data are similar to those calculated from coincident travel time data.

Figure 10 Contour map of the percent sand in shallow soil measurements collected during the detailed studies and during borehole excavation. The locations of the data points used to generate this image are shown in Figure 1. The spatial pattern produced by soil texture is similar to that observed in the water content distribution maps shown in Figures 7-9.

Table 1: Comparison of GPR estimates of water content with conventional measurements

Dependent Variable	Independent Variable	Correlation Coefficient (R)	Linear Regression Equation
θ_v from 900 MHz CMP data	θ_v from gravimetric water content measurements	0.97	θ_v(CMP GPR) = 0.871θ_v(gravimetric) + 0.033
θ_v from 450 MHz CMP data	θ_v from gravimetric water content measurements	0.91	θ_v(CMP GPR) = 0.604θ_v(gravimetric) + 0.092
θ_v from 900 MHz common-offset data	θ_v from gravimetric water content measurements	0.95	θ_v(common-offset GPR) = 0.881θ_v(gravimetric) + 0.041
θ_v from 450 MHz common-offset data	θ_v from gravimetric water content measurements	0.97	θ_v(common-offset GPR) = 0.769θ_v(gravimetric) + 0.067
θ_v from 900 MHz common-offset data	θ_v from TDR	0.94	θ_v(common-offset GPR) = 0.919θ_v(TDR) + 0.040
θ_v from 450 MHz common-offset data	θ_v from TDR	0.97	θ_v(common-offset GPR) = 0.846θ_v(TDR) + 0.054

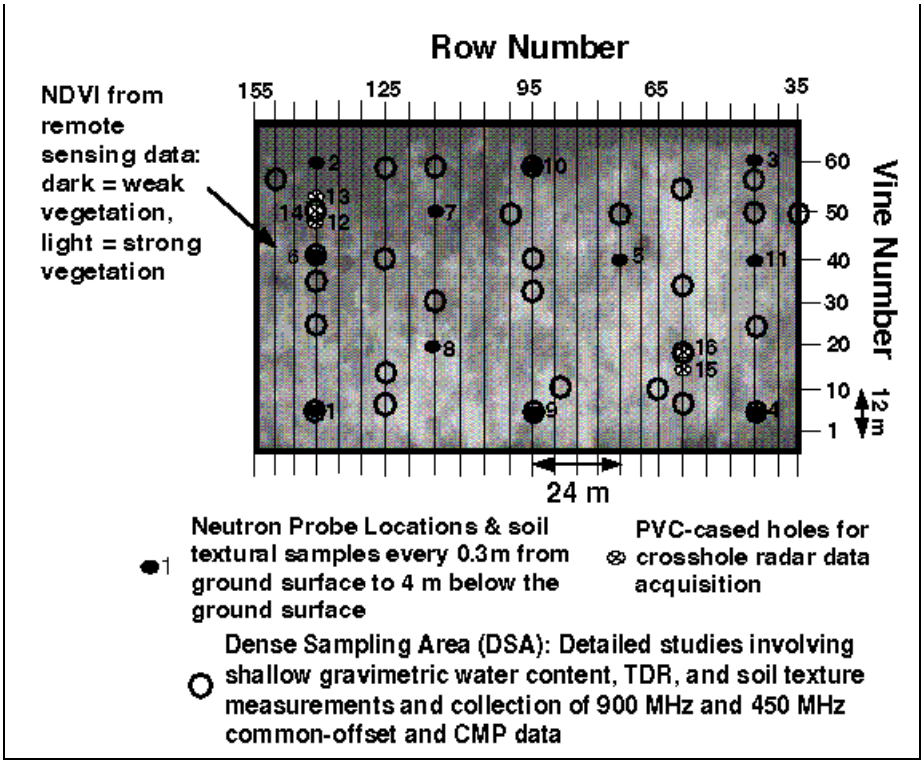
Row Number
155
125
95
65
35
NDVI from remote sensing data: dark = weak vegetation, light = strong vegetation
Vine Number
60
50
40
30
20
10
1
12 m
24 m
Neutron Probe Locations & soil textural samples every 0.3m from ground surface to 4 m below the ground surface
PVC-cased holes for crosshole radar data acquisition
Dense Sampling Area (DSA): Detailed studies involving shallow gravimetric water content, TDR, and soil texture measurements and collection of 900 MHz and 450 MHz common-offset and CMP data

Figure 1

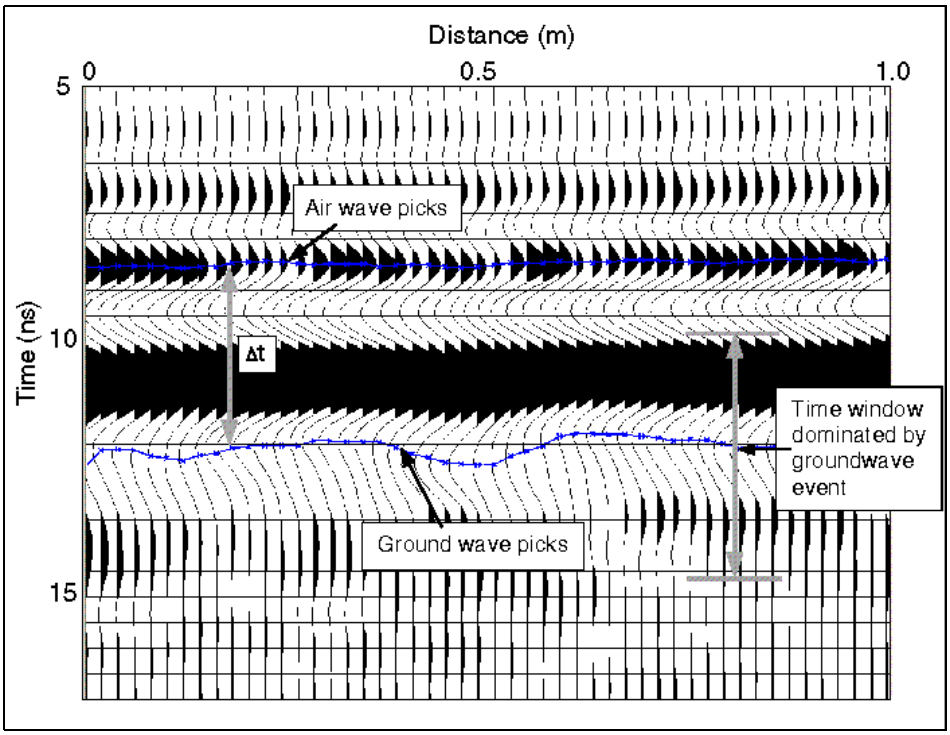
Distance (m)
0
0.5
1.0
Time (ns)
5
10
15
Air wave picks
Δt
Time window dominated by groundwave event
Ground wave picks

Figure 2

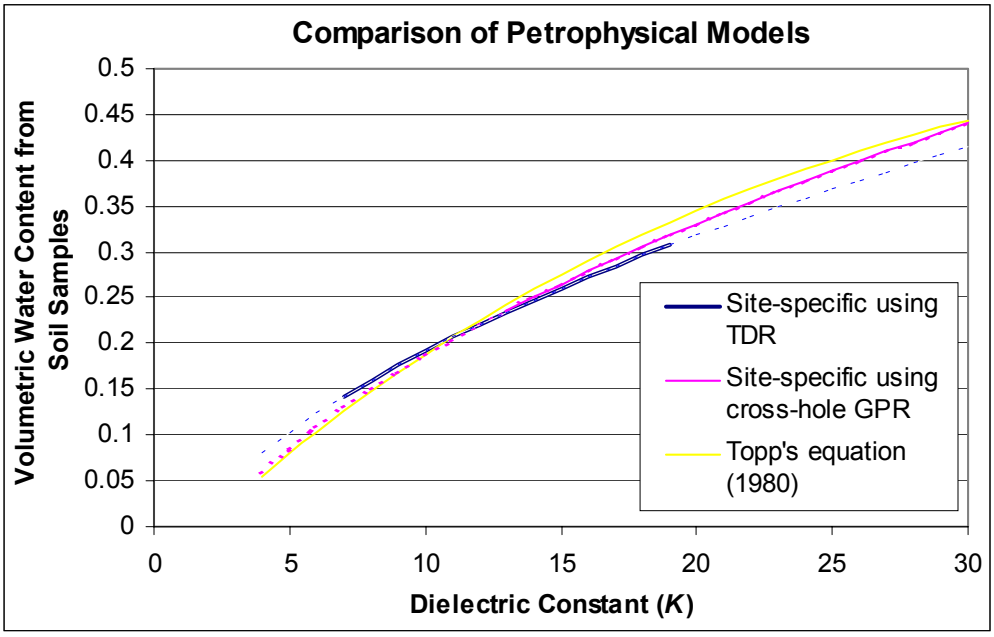

Figure 3

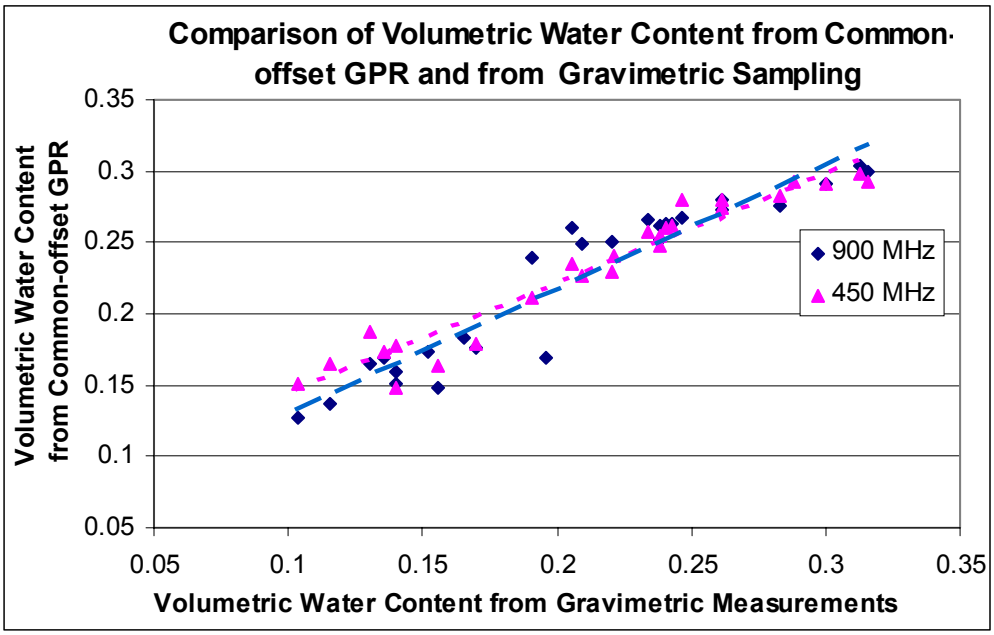

Figure 4

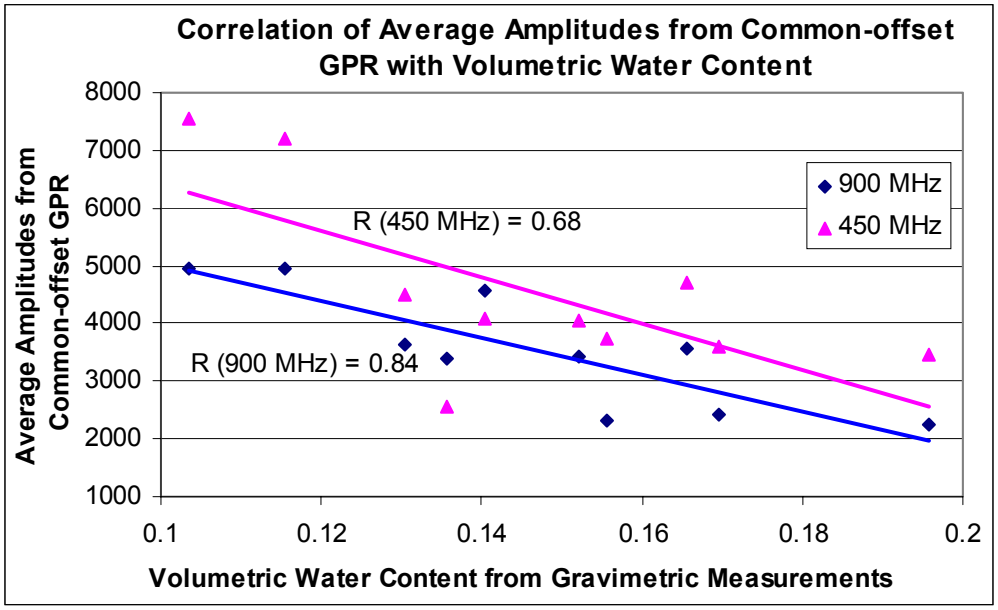

Figure 5

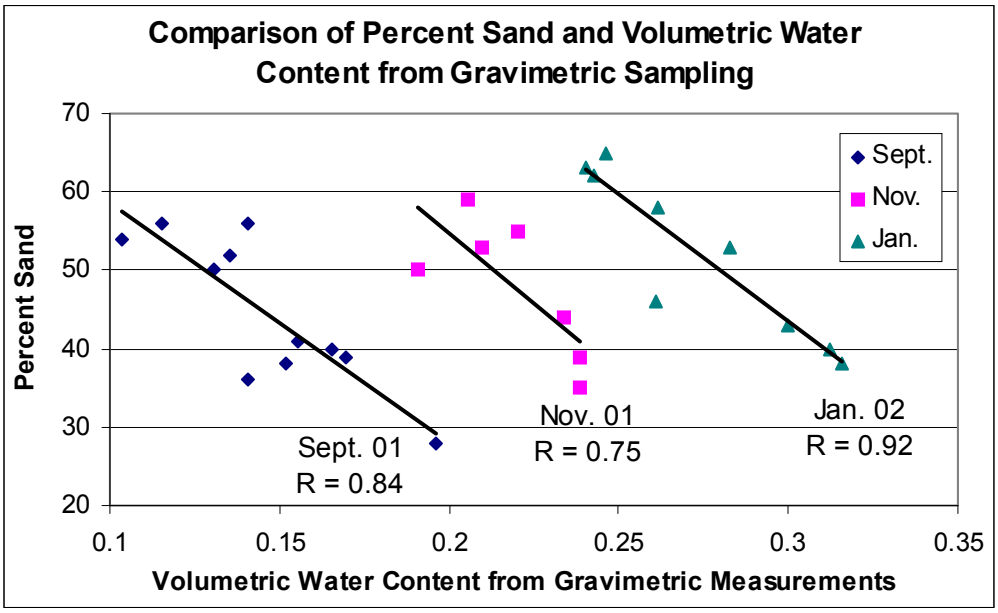

Figure 6

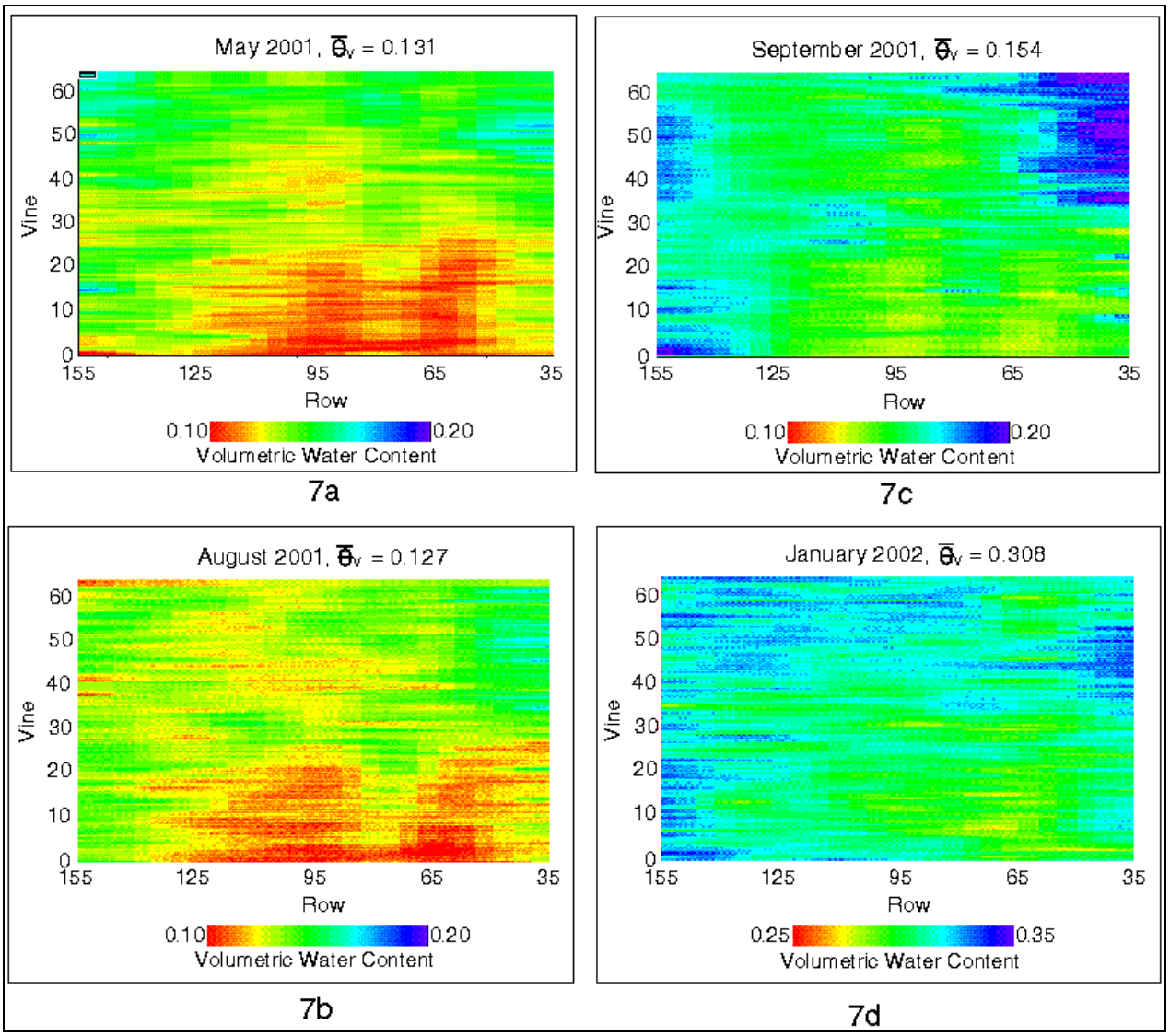
May 2001, $\overline{\theta}_v$ = 0.131
September 2001, $\overline{\theta}_v$ = 0.154
August 2001, $\overline{\theta}_v$ = 0.127
January 2002, $\overline{\theta}_v$ = 0.308
Vine
Row
0.10
0.20
0.25
0.35
Volumetric Water Content
7a
7b
7c
7d

Figure 7

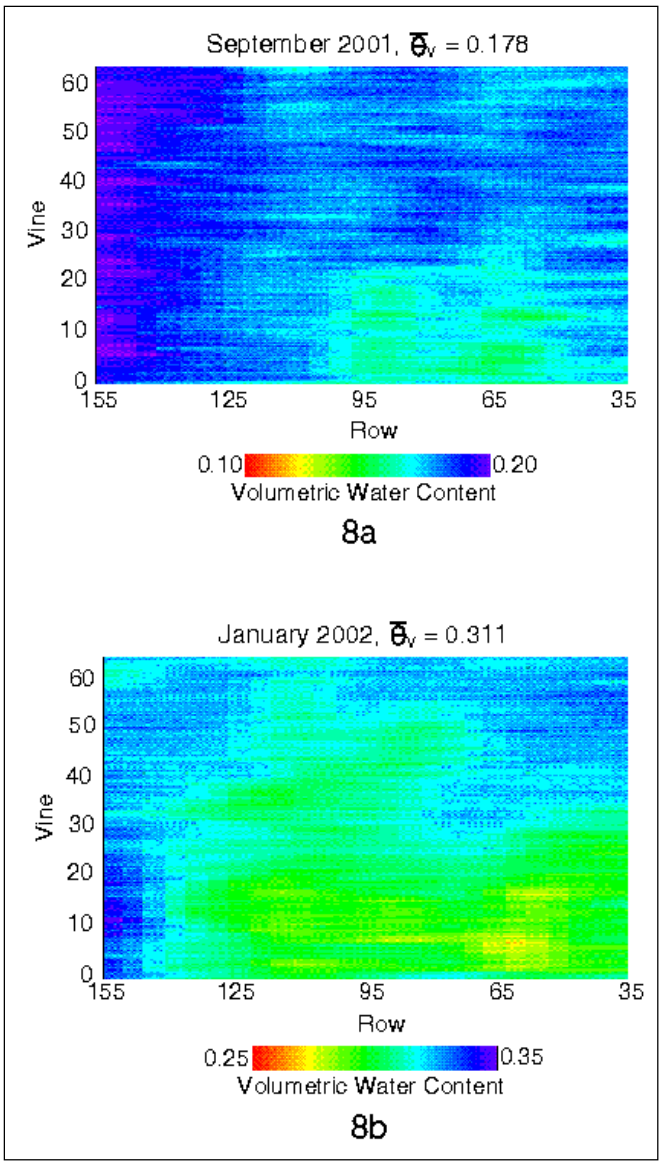

Figure 8

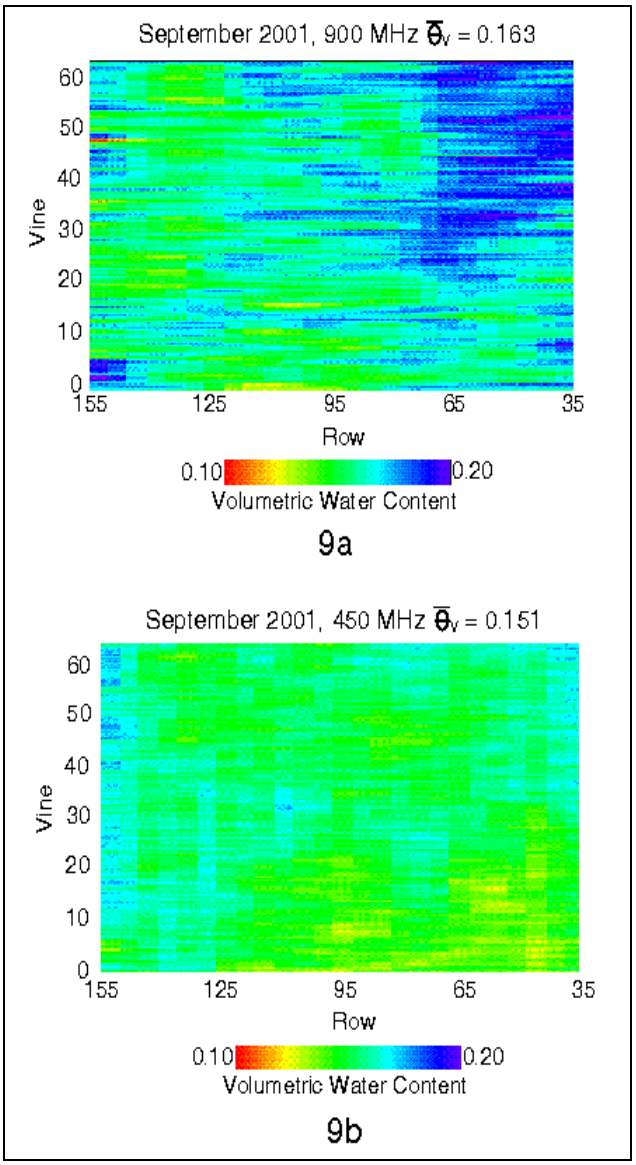

Figure 9

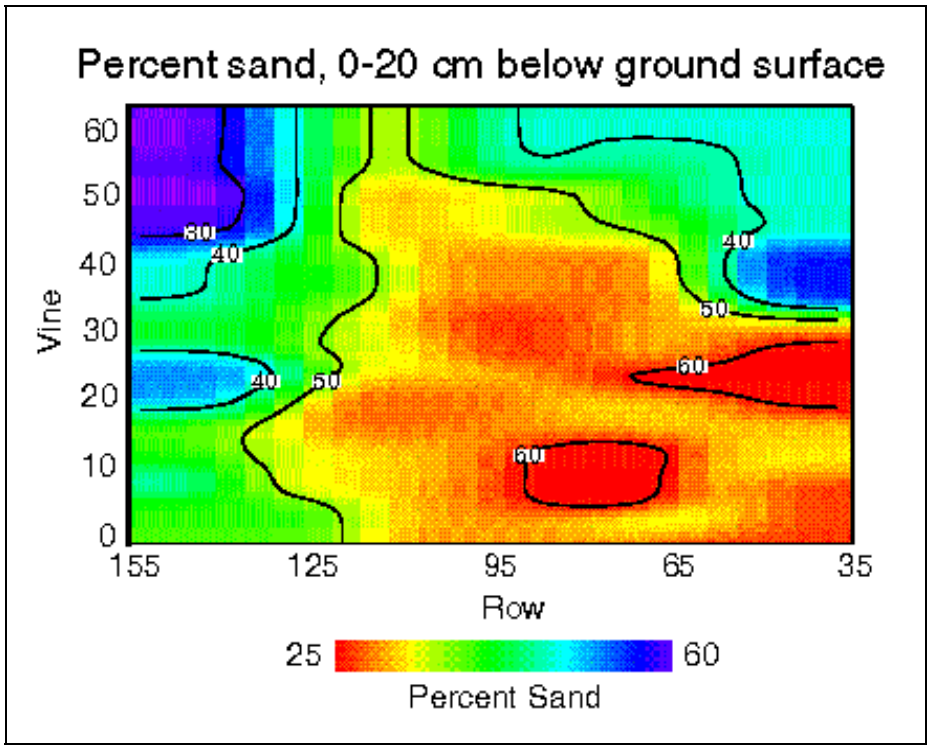
Percent sand, 0-20 cm below ground surface
Vine
60
50
40
30
20
10
0
155
125
95
65
35
Row
60
40
50
25
60
Percent Sand

Figure 10